HHS Public Access

Author manuscript

Immunol Res. Author manuscript; available in PMC 2019 August 01.

Published in final edited form as:

Immunol Res. 2018 August ; 66(4): 445–461. doi:10.1007/s12026-018-9011-x.

RGC-32 regulates reactive astrocytosis and extracellular matrix deposition in experimental autoimmune encephalomyelitis

Alexandru Tatomir[1], **Cosmin A. Tegla**[1,2], **Alvaro Martin**[1], **Dallas Boodhoo**[1], **Vinh Nguyen**[3], **Adam J. Sugarman**[1], **Armugam Mekala**[1], **Freidrich Anselmo**[1], **Anamaria Talpos-Caia**[1,4], **Cornelia Cudrici**[5], **Tudor C. Badea**[6], **Violeta Rus**[2,3], and **Horea Rus**[1,2,7]

[1]Department of Neurology, University of Maryland School of Medicine, 655 W Baltimore St, BRB 12-033, Baltimore, MD 21201, USA

[2]Research Service, Veterans Administration Maryland Health Care System, Baltimore, MD, USA

[3]Department of Medicine, Division of Rheumatology and Clinical Immunology, University of Maryland School of Medicine, Baltimore, MD, USA

[4]Department of Rheumatology, “Iuliu Hatieganu” University of Medicine and Pharmacy, Cluj-Napoca, Romania

[5]National Institute of Arthritis and Musculoskeletal and Skin Diseases, National Institutes of Health, Bethesda, MD, USA

[6]Retinal Circuit Development and Genetics Unit, N-NRL, National Eye Institute, Bethesda, MD, USA

[7]Veterans Administration Multiple Sclerosis Center of Excellence–East, Baltimore, MD, USA

Abstract

Extracellular matrix (ECM) deposition in active demyelinating multiple sclerosis (MS) lesions may impede axonal regeneration and can modify immune reactions. Response gene to complement (RGC)-32 plays an important role in the mediation of TGF-β downstream effects, but its role in gliosis has not been investigated. To gain more insight into the role played by RGC-32 in gliosis, we investigated its involvement in TGF-β-induced ECM expression and the upregulation of the reactive astrocyte markers α-smooth muscle actin (α-SMA) and nestin. In cultured neonatal rat astrocytes, collagens I, IV, and V, fibronectin, α-SMA, and nestin were significantly induced by TGF-β stimulation, and RGC-32 silencing resulted in a significant reduction in their expression. Using astrocytes isolated from RGC-32 knock-out (KO) mice, we found that the expression of TGF-β-induced collagens I, IV, and V, fibronectin, and α-SMA was significantly reduced in RGC-32 KO mice when compared with wild-type (WT) mice. SIS3 inhibition of Smad3 phosphorylation was also associated with a significant reduction in RGC-32 nuclear translocation and TGF-β-induced collagen I expression. In addition, during experimental

Electronic supplementary material The online version of this article (https://doi.org/10.1007/s12026-018-9011-x) contains supplementary material, which is available to authorized users.

Compliance with ethical standards

Conflict of interest

H.R. has received a grant from TEVA Neuroscience (CNS-2014–174). All other authors declare that they have no conflict of interest.

autoimmune encephalomyelitis (EAE), RGC-32 KO mouse astrocytes displayed an elongated, bipolar phenotype, resembling immature astrocytes and glial progenitors whereas those from WT mice had a reactive, hypertrophied phenotype. Taken together, our data demonstrate that RGC-32 plays an important role in mediating TGF-β-induced reactive astrogliosis in EAE. Therefore, RGC-32 may represent a new target for therapeutic intervention in MS.

Keywords

RGC-32; Astrocyte; Multiple sclerosis; Experimental autoimmune encephalomyelitis; Extracellular matrix

Introduction

We have previously identified Response Gene to Complement (RGC)-32 as a novel gene product that is induced by complement activation and have demonstrated its activity, primarily as a cell cycle regulator [1]. We have also shown that overexpression of RGC-32 leads to an increase in DNA synthesis and causes cell cycle progression from the G1/G0 to the G2/M phase [2]. Both of these responses can be abolished by silencing RGC-32 expression with specific siRNA [3, 4]. Thus, RGC-32 appears to be a previously unrecognized regulator of Akt and CDC2 (cell division cycle protein 2 homolog), critical kinases involved in cell cycle regulation. RGC-32 protein forms complexes with CDC2/cyclin B1 and enhances CDC2 kinase activity [2]. In addition, RGC-32 binds and modulates the activity of Akt [4].

Since complement activation induces RGC-32 expression and is also involved in the pathogenesis of multiple sclerosis (MS) lesions [5], we asked how RGC-32 might play a role in MS. Our previous studies have shown that $CD3^+$, $CD68^+$, and glial fibrillary acidic protein (GFAP)-positive cells in MS plaques express RGC-32 [6]. In addition, we have reported that RGC-32 is preferentially upregulated during Th17 cell differentiation. RGC-$32^{-/-}$ mice have normal Th1, Th2, and regulatory T-cell differentiation but show defective Th17 differentiation in vitro. This impaired Th17 differentiation is associated with defects in IFN regulatory factor 4, B cell–activating transcription factor, retinoic acid–related orphan receptor γt, and SMAD2 activation [7]. In vivo, RGC-$32^{-/-}$ mice display an attenuated experimental autoimmune encephalomyelitis (EAE) phenotype, accompanied by decreased CNS inflammation and a reduced frequency of IL-17- and GMCSF-producing $CD4^+$ T cells. These studies have identified RGC-32 as a novel regulator of Th17 cell differentiation in vitro and in vivo and suggest that RGC-32 is a potential therapeutic target in multiple sclerosis [7]. Since RGC-32 is also expressed by astrocytes in MS lesions, its role in these cells needs to be explored.

Studies investigating the development of excess fibrous connective tissue and the repair process in various organs have reported a consistent pattern of RGC-32 upregulation [8]. In addition, it was recently demonstrated that RGC-32 is induced by TGF-β and plays a critical role in the TGF-β-induced epithelial–mesenchymal transition (EMT) of renal tubular cells [9, 10]. Overall, these data point to the possibility that RGC-32 plays an active part in the processes of scar development and wound healing.

The formation of glial scars sits at the extreme endpoint on an axis of various morphological and molecular changes that astrocytes can undergo as a result of all forms of CNS injury, including inflammation, and which are collectively called reactive astrogliosis [11–13]. Morphologically, the reactive astrocyte shows hypertrophy of its cell body and processes. Reactive astrogliosis can be reversible in its mild and moderate forms, but it can become irreversible if the CNS injury is severe and persistent. In this case, as in chronic MS lesions, astrocytes can enter a proliferative state and contribute to the formation of a glial scar by producing and leading to the deposition of extracellular matrix (ECM) [11, 14].

Given the important role of RGC-32 in fibrosis, it seems reasonable to investigate its role in gliosis. The relationship between RGC-32 and TGF-β-mediated gliosis in EAE and MS has not been explored in detail. In this paper, we further investigated the role of RGC-32 in mediating TGF-β-induced reactive astrogliosis and ECM synthesis. Using in vitro cell cultures and an RGC-32 knockout (KO) mouse model, we show that RGC-32 plays an important role in mediating TGF-β effects on both reactive astrocyte markers and ECM production. These effects are mediated by a physical interaction of RGC-32 with Smad3, as shown by co-immunoprecipitation and nuclear translocation assays. In addition, immunohistochemical analysis of spinal cords from mice with EAE showed that the astrocytes from RGC-32 KO mice display an elongated phenotype with long processes, whereas the astrocytes from wild-type (WT) mice display a reactive astrocyte phenotype with body hypertrophy. Taken together, our data demonstrate that RGC-32 plays an important role in the mediation of TGF-β-induced reactive astrogliosis in EAE.

Materials and methods

Brain tissue

Frozen brain tissue specimens acquired at autopsy from seven patients with a definitive diagnosis of MS were obtained from the Human Brain and Spinal Fluid Resource Center, Veterans Affairs West Los Angeles Health Care Center. Active lesions contained abundant infiltrates consisting of T cells and macrophages, with detectable myelin degradation products. Inflammation was restricted to the lesion margins in chronic active lesions. Regions of normal-appearing white matter (NAWM) and normal-appearing gray matter (NAGM) lesions that lacked macroscopic or histological evidence of demyelination were also used. The samples were derived from patients between the ages of 38 and 51, with a mean age of 47. Brain samples acquired at autopsy from six healthy control individuals between the ages of 36 and 72 (mean age, 49) were obtained from the Cooperative Human Tissue Network, Charlottesville, VA.

Induction and evaluation of EAE

RGC-32 KO and WT female mice (8–10 weeks old) were injected subcutaneously in two locations in the dorsal flank with an emulsion containing 200 μg of $MOG_{35–55}$ (Anaspec, Fremont, CA) and complete Freund's adjuvant (CFA) (Difco, Detroit, MI) as previously described [7, 15]. Pertussis toxin (400 ng; List Biological Laboratories, Campbell, CA) was administered intraperitoneally on days 0 and 2. Mice were monitored daily, and the disease was scored on a scale of 0–5 as follows: 1, limp tail; 2, hindlimb paresis; 3, hindlimb

paralysis; 4, tetraplegia; 5, moribund [7, 15]. All procedures were approved by the University of Maryland School of Medicine Office of Animal Welfare Assurance.

Immunohistochemical staining

MS samples—Cryostat sections (5 μm) of MS brains were air-dried and fixed in acetone for 10 min. The sections were washed in PBS, and endogenous peroxidase was quenched with 0.3% hydrogen peroxide in PBS for 10 min. The slides were then incubated overnight at 4°C with the following primary antibodies: rabbit IgG anti-collagens I–III (Santa Cruz Biotechnology, Dallas, TX), rabbit IgG anti-collagen IV (Bioss Antibodies, Woburn, MA), rabbit IgG anti-collagen V (Rockland, Pottstown PA), or mouse IgG anti-fibronectin (Thermo Scientific, Waltham, MA), then washed with PBS and processed with an R.T.U. Vectastain Universal Quick Kit (Vector Labs, Burlingame, CA) as previously described [16]. The reactions were developed using Nova RED (Vector Labs) as the chromogen substrate, and the sections were then washed in distilled water and counterstained with Harris hematoxylin (Sigma-Aldrich, St. Louis, MO), dehydrated, mounted, and scored by two observers in a blinded fashion. Control sections were prepared by immunostaining without the primary antibody.

EAE samples—Cryostat sections (5 μm) of spinal cord were air-dried and fixed in acetone for 10 min. They were then washed in PBS, and endogenous peroxidase was quenched with 0.3% hydrogen peroxide in PBS for 10 min. The slides were incubated overnight at 4°C with the primary antibody, rabbit IgG anti-RGC-32 (Bioss Antibodies), then washed with PBS and incubated with biotinylated goat anti-rabbit IgG (Jackson ImmunoResearch Labs, West Grove, PA) followed by an R.T.U. streptavidin–peroxidase complex (Vector Labs). The reactions were developed using Nova RED (Vector Labs) as the chromogen substrate. For GFAP immunostaining, paraffin-embedded spinal cords were prepared as previously described [17] and treated with Bloxall (Vector Labs) to inhibit endogenous alkaline phosphatase. They were then incubated with rabbit IgG anti-GFAP (Dako Agilent, Santa Clara, CA) overnight at 4°C and then with goat alkaline phosphatase anti-rabbit IgG (Vector Labs) for 1 h at room temperature. The reactions were developed using a Vector alkaline phosphatase substrate kit III (Vector Labs) as the chromogen substrate.

Double-staining immunohistochemistry

MS brains—Frozen sections (5 μm) from the brains of adult patients with MS were double-stained for collagen I, IV, or V and for GFAP as previously described [6]. Cryosections were initially treated with Bloxall (Vector Labs) to remove endogenous peroxidase and alkaline phosphatase, then incubated with primary antibodies against collagen I, IV, or V as described above, and the reaction was developed with Nova RED (Vector Labs) for collagen I and RGC-32 or Vector alkaline phosphatase substrate kit III (Vector Labs) for collagens IV and V. The sections were then incubated overnight with mouse IgG anti-GFAP monoclonal antibody (eBioscience, San Diego, CA). The slides were washed several times in PBS and reacted with alkaline phosphatase-conjugated goat anti-mouse (Sigma-Aldrich), diluted 1/400 and processed with Vector alkaline phosphatase substrate kit III (Vector Labs) or Nova RED as the chromogen substrate.

Astrocyte isolation

Neonatal astrocytes were purified from the brains of 1-day-old Sprague–Dawley rat pups and of RGC-32$^{-/-}$ and WT mouse pups as previously described [18]. After removal of the meninges, the brains were minced and sequentially passed through nylon meshes. The resulting cell suspensions were plated onto 75-cm^2 plates in DMEM/Ham's F-12 medium containing 10% FBS. Oligodendrocyte precursor cells (OPC) and glial cells were separated from the astrocyte mono-layer by shaking overnight at 200 rpm on a rotary shaker. The OPC/glial cell suspension was discarded, and adherent astrocytes were kept in DMEM/Ham's F-12 medium containing 10% FBS. More than 97% of the cells isolated expressed the astrocyte marker GFAP.

Transfection of astrocytes

Rat astrocytes were transiently transfected with RGC-32 siRNA (siRGC-32) or control siRNA (siCTR) (Santa Cruz Biotechnology) by using Lipofectamine 3000 (Invitrogen, Carlsbad, CA): 75 pmol of siRNA and 7.5 μl of Lipofectamine 3000 were diluted separately in Opti-MEM I Reduced Serum Medium (Gibco, Waltham, MA), incubated for 5 min at room temperature, then combined and incubated for 10 min at room temperature. At 24 h after transfection, the astrocytes were changed into DMEM/Ham's F-12 supplemented with 10% FBS for another 24 h, then starved in serum-free DMEM overnight and treated with 10 ng/ml TGF-β (Gibco) or vehicle for the indicated periods of time.

RNA isolation, cDNA synthesis, and quantitative real-time PCR

Total RNA from astrocytes was purified using an RNeasy Mini Kit (Qiagen, Germantown, MD) according to the manufacturer's instructions. RNA (0.5 μg) was reverse-transcribed to obtain cDNA. Forward and reverse primers for RGC-32, COL1A1, COL4A1, COL5A1, FN1, nestin, and ACTA2 were provided by IDT (Coralville, IA) (Supplemental Table 1). Real-time PCR was performed according to the manufacturer's protocol using a FastStart Universal SYBR Green Master mix (Roche, Indianapolis, IN) and StepOnePlus Real Time PCR System (Applied Biosystems, Carlsbad, CA). Quantification was performed by using the ΔΔCT method of relative quantification as previously described [15].

Nuclear/cytoplasmic extract preparation

To prepare nuclear and cytoplasmic extracts, we used a NEPER kit (Thermo Scientific). In brief, cells were washed with PBS, trypsinized, resuspended in cytoplasmic extraction reagent I (CER I), and incubated on ice. Cytoplasmic extraction reagent II (CER II) was then added, and the extracts were further incubated on ice. The extracts were centrifuged for 5 min, and the cytoplasmic fraction was transferred to a new tube. Nuclear extraction reagent (NER) was added to the pellet, and the nuclear pellet was incubated on ice for 40 min, with vortexing every 10 min. The extract was then centrifuged for 10 min, and the nuclear fraction was transferred to a new tube. Samples of nuclear and cytoplasmic extracts were further processed by Western blotting.

Co-immunoprecipitation assay

Cells were lysed in 500 μl co-immunoprecipitation assay (co-IP) lysis buffer (Thermo Scientific) on ice for 30 min. The protein extracts were incubated with anti-IgG, -Smad2, -Smad3, or -Smad4 antibodies at 4°C for 2 h, followed by the addition of 10 μl protein A/G-agarose beads (Santa Cruz Biotechnology) and incubation at 4°C overnight. Immunoprecipitates were washed three times with RIPA buffer and then resuspended and boiled in SDS loading buffer. Western blotting was performed using an anti-RGC-32 antibody generated by us [19].

Western blotting

Western blotting was performed as previously described [6, 20]. For total protein extraction, cells were lysed in RIPA lysis buffer containing protease and phosphatase inhibitors. The primary antibodies were rabbit IgG anti-collagen I, V (Rockland), or IV (Bioss Antibodies); rabbit IgG anti-fibronectin (Proteintech, Chicago, IL); rabbit IgG anti-α-SMA (GeneTex, Irvine, CA); mouse IgG anti-nestin (Santa Cruz Biotechnology); rabbit IgG anti-phospho-SMAD3 (pS423 pS435) (Rockland, PA); rabbit IgG anti-SMAD2, SMAD3, and SMAD4 (Cell Signaling Technology, Danvers, MA); and rabbit IgG anti-RGC-32 [6]. The secondary antibodies were goat anti-rabbit or anti-mouse IgG-HRP (Santa Cruz Biotechnology). Immune complexes were detected using enhanced chemiluminescence (Denville Scientific Inc., Holliston, MA). The density of the bands was measured using UN-SCAN-IT software, version 7.1 (Silk Scientific Inc., Orem, UT).

Statistical analysis

Comparisons between two groups were performed using unpaired two-tailed Student's t test. Comparisons between multiple groups were performed using one-way or two-way ANOVA with Bonferroni correction. p values < 0.05 were considered significant. Statistical analysis was performed using Graph Pad software, version 7. All values are shown as means ± SEM and are representative of three experiments unless otherwise noted.

Results

RGC-32 and ECM components are expressed in MS lesions

One important question to answer was whether ECM expression was higher in MS brains than in controls. Therefore, we examined the expression of collagen I (Fig. 1a), collagen II (Fig. 1b), collagen III (Fig. 1c), collagen IV (Fig. 1d), collagen V (Fig. 1e), and fibronectin (Fig. 1f) by immunostaining of MS brains (Table 1). Collagens I–V and fibronectin were found to be localized around the blood vessels and in the parenchyma. These ECM components were present in significantly higher amounts in MS plaques, NAWM, and NAGM (Table 1) than in control brains (Fig. 1g, h). In active MS lesions, collagens I, III, IV, and V were found around blood vessels, in the perivascular space (PVS), and in parenchymal areas outside the PVS. In contrast, control brain tissue showed a faint staining for the ECM components studied here, mainly around the blood vessels (Table 1). An example of staining for collagen I and III deposits in the blood vessels of normal brain is shown in Fig. 1g and h. Statistically significant higher levels of scores for ECM components

staining intensities were found in MS brain when compared to control brain (Supplemental Fig. 1). Controls for the immunoperoxidase reaction were negative (Fig. 1i).

Co-localization of collagens I, IV, and V with GFAP

Previous work has concluded that most of ECM is produced by inflammatory infiltrates [21]. Since we were interested in the role of RGC-32 in ECM production by astrocytes, we next investigated the co-localization of $GFAP^+$ astrocytes with collagens I, IV, and V. We found that collagen I (Fig. 2a), collagen IV (data not shown), and collagen V (Fig. 2b) were co-localized with $GFAP^+$ astrocytes in perivascular and parenchymal areas. Taking into account the observation that RGC-32 was also found to be co-localized with $GFAP^+$ astrocytes (Fig. 2c), these data suggest that RGC-32 might regulate ECM production in vivo. Controls for the immunoperoxidase reaction were negative (Fig. 2d).

TGF-β induces the expression of RGC-32 in astrocytes

To further investigate the expression of RGC-32, we cultured primary rat astrocytes and stimulated them with TGF-β (10 ng/ml) for the indicated periods of time. We examined the expression of RGC-32 mRNA by real-time PCR and protein by Western blotting. Our data show that both RGC-32 mRNA and protein expressions were significantly increased over unstimulated cells at 18 h ($p = 0.01$, Fig. 3a) and 24 h, respectively ($p < 0.0001$, Fig. 3b), indicating that TGF-β induces RGC-32 expression in astrocytes.

TGF-β induces the expression of collagens I, IV, and V, fibronectin, α-smooth muscle actin (α-SMA), and nestin in astrocytes

Next, we investigated the mRNA expression of $\alpha 1$ chains of collagen type I (COL1A1), type IV (COL4A1), and type V (COL5A1) and fibronectin (FN1) after stimulation with TGF-β (10 ng/ml) by using real-time PCR. We found a statistically significant increase in the expression of all these ECM components after 18 h of stimulation ($p < 0.0001$ for COL1A1, $p = 0.007$ for COL4A1, $p = 0.03$ for COL5A1, $p = 0.02$ for FN1) (Fig. 4a). In addition to ECM components, we investigated the TGF-β-mediated induction of the mRNAs of reactive astrocyte markers α-smooth muscle actin (ACTA2) and nestin [22]. Both ACTA2 ($p = 0.01$) and nestin ($p = 0.004$) were significantly increased at 18 h of stimulation (Fig. 4b). The protein levels of collagen I, collagen IV, collagen V, fibronectin, α-SMA, and nestin were also significantly induced by TGF-β at 24 h of stimulation (Fig. 5). These data suggest that TGF-β induces both astrocyte transition to a reactive state and the production of ECM.

The effect of RGC-32 silencing on the TGF-β-induced ECM components and reactive astrocyte markers

To investigate the possible role of RGC-32 in mediating these TGF-β effects, we silenced RGC-32 expression in cultured rat astrocytes by using specific RGC-32 siRNA. After TGF-β stimulation, both RGC-32 mRNA ($p < 0.02$, Fig. 6a) and protein levels ($p < 0.0001$, Fig. 6b) were significantly reduced when compared to siCTR. RGC-32 silencing significantly reduced the TGF-β-induced mRNA expression of COL1A1 ($p = 0.03$), COL4A1 ($p = 0.03$), COL5A1 ($p = 0.04$), and FN1 ($p = 0.01$) (Fig. 6c). In addition, ACTA2 ($p = 0.04$) and nestin ($p = 0.009$) mRNAs were also significantly reduced after RGC-32 silencing when compared

with siCTR (Fig. 6d). A similar reduction was seen in the protein levels of collagen I ($p < 0.007$), collagen V ($p = 0.02$), fibronectin ($p = 0.02$), α-SMA ($p < 0.05$), and nestin ($p < 0.05$) (Fig. 7). These data suggest that RGC-32 plays an important role in TGF-β-mediated ECM production and the expression of reactive astrocyte markers.

The effect of TGF-β on ECM components and α-SMA expression in RGC-32 KO mouse astrocytes

To further investigate the effects of RGC-32 silencing on TGF-β-induced ECM and reactive astrocyte markers, we used primary astrocyte cultures obtained from RGC-$32^{-/-}$ mice and compared the effects of TGF-β stimulation with those seen in RGC-$32^{+/+}$ astrocytes. We found that the TGF-β-induced mRNA expression of COL1A1 ($p = 0.01$), COL4A1 ($p = 0.0002$), COL5A1 ($p = 0.006$), and ACTA2 ($p = 0.01$) was significantly reduced in the RGC-$32^{-/-}$ mouse astrocytes at 24 h when compared to WT astrocytes (Fig. 8a–d). Similar data were obtained when collagen I, collagen IV, collagen V, and fibronectin protein expression was analyzed (Fig. 8e). Interestingly, the expression of collagens I and IV was almost undetectable and that of fibronectin was also very low in RGC-$32^{-/-}$ astrocytes after stimulation with TGF-β (Fig. 8e). These data suggest that RGC-32 may play a similar role in mouse astrocytes in mediating TGF-β effects. In addition, it seems that the lack of RGC-32 has a greater effect on the TGF-β-induced expression of collagens I, IV, and fibronectin than on that of the other ECM components examined here.

RGC-32 interacts with Smad3 and is transferred to the nucleus

RGC-32, a TGF-β downstream target, plays an essential role in the TGF-β-induced epithelial-to-mesenchymal transition (EMT) [10] and affects connective tissue matrix proteins in astrocytes [6]. The mechanisms underlying RGC-32 function, however, remain largely unknown. Receptor-activated Smad2 and Smad3 (R-Smad) proteins, together with the common mediator Smad4, are central components of TGF-β signaling pathways [23]; therefore, we asked whether RGC-32 interacts with Smad2 or Smad3 in astrocytes. To look for physical interaction between RGC-32 and Smad3, we performed co-IP using endogenous proteins extracted from rat astrocytes that had been stimulated with TGF-β. Anti-Smad3 antibody specifically pulled down RGC-32, suggesting that RGC-32 interacts with Smad3 after TGF-β treatment (Fig. 9). RGC-32 did not co-immunoprecipitate with either Smad4 or Smad2 (data now shown), suggesting that RGC-32 does not physically interact with either of these proteins.

Next, we examined the nuclear translocation of RGC-32 and Smad3 after stimulation with TGF-β. As expected, stimulation of rat astrocytes with TGF-β induced the nuclear translocation and phosphorylation of Smad3 (Fig. 10a–c). Moreover, RGC-32 was also translocated to the nucleus (Fig. 10a, d). To determine whether Smad3 phosphorylation is required for RGC-32 nuclear translocation, we treated astrocytes with SIS3, a specific and potent inhibitor of Smad3 phosphorylation [24]. SIS3 treatment resulted in a significant reduction in TGF-β-induced phosphorylated Smad3 ($p < 0.001$) and total Smad3 ($p < 0.01$) levels in the nuclear fraction and a significant reduction in RGC-32 translocation to the nucleus ($p < 0.0001$), indicating that Smad3 phosphorylation is required for RGC-32's

translocation to the nucleus (Fig. 10a–d). SIS3 inhibition of Smad3 phosphorylation was also associated with a reduction in TGF-β-induced collagen I expression (Fig. 10e).

Since the RhoA-Rho kinase (ROCK) signaling module was previously shown to be a modulator of Smad signaling [25], we investigated the possible effect of ROCK inhibition on Smad3/RGC-32 nuclear translocation by using a cell-permeable, highly potent and selective ROCK inhibitor (Y27632). ROCK inhibition significantly reduced TGF-β-induced RGC-32 nuclear translocation but had no effect on that of Smad3 (Fig. 10f), suggesting that ROCK is also required for the translocation of RGC-32 to the nucleus in astrocytes. On the other hand, RGC-32 silencing with siRGC-32 did not significantly influence the translocation of Smad3 to the nucleus (Fig. 10g).

RGC-32 deficiency attenuates EAE and affects the astrocyte phenotype

To evaluate the effect of RGC-32 on astrocytes in an autoimmune inflammatory condition, we induced EAE in WT and RGC-32$^{-/-}$ mice by immunization with $MOG_{35–55}$. As previously reported, RGC-32$^{-/-}$ mice developed significantly less severe disease at the stage of peak disease [7] (Fig. 11a). The attenuated EAE phenotype was confirmed by histopathological examination of the spinal cords, which showed fewer inflammatory infiltrates and demyelination foci in RGC-32$^{-/-}$ mice than were seen in WT mice (Fig. 11b, c). The score for inflammation in RGC-32$^{-/-}$ was decreased to 0.8 ± 0.1 ($p < 0.0001$) when compared with WT mice (2.4 ± 0.18) (Fig. 11d). In addition, during EAE at peak of the disease (day 14), RGC-32$^{-/-}$ astrocytes displayed an elongated, radial, or bipolar phenotype, with the astrocytic processes oriented mostly perpendicular to the lesional area, whereas those in WT mice displayed a reactive astrocyte phenotype with body hypertrophy (Fig. 12). These data suggest a role for RGC-32 in the differentiation of astrocytes to a reactive phenotype in vivo during inflammatory conditions.

Discussion

>TGF-β signaling plays a critical role in gliosis [24–27]. The molecular mechanisms underlying TGF-β function in gliosis remain largely unknown. Our data from the current study provide significant detailed insights into RGC-32-mediated ECM production by astrocytes and the involvement of this phenomenon in multiple sclerosis and its experimental model, EAE. Previous studies have demonstrated that the TGF-β downstream target gene RGC-32 is important for induction of mRNA of collagen I, fibronectin, and α-SMA in astrocytes [6]. We now show that mRNA and protein expression of collagens I, V, and fibronectin, together with those of α-SMA and nestin, are induced by TGF-β and regulated by RGC-32 in rat astrocytes. The TGF-β-induced expression of collagens I, IV, and V, fibronectin, and α-SMA were also significantly reduced in RGC-32$^{-/-}$ mice when compared to WT mice. Our results concerning collagen I and fibronectin are of particular importance since these molecules are major components of the ECM, and their deposition is increased in gliotic lesions [21, 28]. Collagen type I and type IV, together with fibronectin, were not induced at all by TGF-β in RGC-32$^{-/-}$ mouse astrocytes. Mutations of the COL1A1 gene leading to defective collagen I in the connective tissue are associated with various diseases of the skin, bones, and tendons, such as Ehlers–Danlos syndrome and osteogenesis

imperfecta in humans [26], and COL1A1 KO mice show various phenotypes, ranging from embryonic lethality to impaired bone formation, increased bone fragility, and fatal aortic dissection [27]. Nevertheless, collagen I seems critical for the formation of the glial scar [29]. Type IV collagen is expressed particularly in basement membranes and is an important component of the glial scar [28]. It may also have a major role in inhibiting neurite outgrowth during glial scar formation [30]. Our data also support earlier observations that reactive astrocytes are a major source of TGF-β-induced type IV collagen [30]. Type V collagen is a fibrillary collagen that has been shown to be upregulated in active MS lesions [21]. Fibronectin is also upregulated in glial scars (Fig. 1 and [31]), and it has been shown to enhance astrocyte proliferation in these scars [32].

Previous studies of MS brains have shown that the fibrillary collagens, biglycan, and decorin are largely found between the endothelium and astrocytic glia limitans in the perivascular space, where they form a meshwork that is closely associated with infiltrating immune cells [21]. In our study, we also found significant deposits of collagens I–Vand fibronectin in MS lesions. In addition, we found that the increased deposition of these extracellular deposits was not confined to the MS plaques but was also present in areas of NAWM and NAGM. Our study has also clearly shown that astrocytes co-localize with collagens, indicating that these cells are an important source of the collagen deposits seen in MS lesions. Previously, an increase in TGF-β was reported in inactive and active MS lesions [33]. The increase in TGF-β levels in MS lesions may trigger the production of ECM components in part by activating RGC-32. Perivascular fibrosis is a typical feature of chronic lesions and may function as both a physical and a biological barrier that limits immune cell recruitment and the expansion of MS lesions [12].

RGC-32 physically interacts with Smad3 to regulate the expression of ECM in astrocytes. RGC-32 and Smad3 also cooperatively regulate the activation of the expression of the reactive astrocyte markers α-SMA and nestin. These data suggest that RGC-32 plays an important role in mediating the astrocytes' transition to a reactive state as well as TGF-β-induced ECM production. TGF-β signaling is mediated by both Smad2 and Smad3 [10, 34], but RGC-32 appears to interact only with Smad3 in inducing ECM production; our coimmunoprecipitation data indicate that RGC-32 does not physically interact with Smad2 in astrocytes (data not shown). A similar interaction has been shown to mediate the EMT of human renal proximal tubular cells [10].

Interestingly, TGF-β induced the nuclear translocation of both Smad3 and RGC-32 in astrocytes. Smad3 is known to be translocated into nuclei in conjunction with Smad4 [23]. However, Smad4 appears to have no role in RGC-32's nuclear translocation because in Smad4-null cells, TGF-β-induced RGC-32 was also found in the nuclei [10]. Moreover, our study demonstrated that the activation of ROCK is also necessary for RGC-32 nuclear localization, but it does not seem to influence Smad3 translocation. Therefore, the nuclear location mechanism for RGC-32 might be differently regulated from that of Smad3, although RGC-32 interacts with Smad3 to regulate ECM production. A previous study has shown that RGC-32 can be phosphorylated by p34CDC2-cyclin B1 in vitro [2], but it is unclear whether this phosphorylation contributes to RGC-32's nuclear localization in vivo or whether RGC-32 is translocated with the cdc2/cyclin B1 complex. Further work is needed to

clarify the mechanism(s) governing RGC-32's nuclear localization. Taken together, our data provide novel information about the mechanism underlying RGC-32 induction of the ECM in both EAE and MS (Fig. 13).

In the present study, we have also shown for the first time that during EAE, inflammatory cells and astrocytes express RGC-32. RGC-32 was previously shown to co-localize with $CD3^+$, $CD68^+$, and $GFAP^+$ cells in MS brains [6]. In addition, we have demonstrated for the first time that RGC-32 can influence the astrocytic phenotype in vivo during EAE, suggesting that RGC-32 plays an important role in the differentiation of astrocytes in an inflammatory milieu. These data, in conjunction with previous reports of a role for RGC-32 in the differentiation of Th17 cells [7] and monocytes [35], suggest a broader role for this protein in cellular differentiation during inflammatory conditions.

Reactive astrocytes are responsible in part for the production of the ECM that accumulates in gliotic areas, a typical feature of chronic lesions. The glial scar may function as both a physical and biological barrier that limits immune cell recruitment and the expansion of MS lesions [11, 21], but it can also have a blocking effect on axonal regeneration and remyelination [36, 37]. In addition, the astrocytic reaction can exert protective effects by reconstituting the blood–brain barrier and preventing neuronal degeneration [38]. In conclusion, our data strongly suggest that RGC-32 represents a potential new target for therapeutic intervention in chronic progressive MS.

Supplementary Material

Refer to Web version on PubMed Central for supplementary material.

Acknowledgments

We thank Dr. Deborah McClellan for editing this manuscript.

Funding

This work was supported in part by Veterans Administration Merit Award I01BX001458 (to H.R.).

Abbreviations

ACTA2	alpha smooth muscle actin
COL1A1	collagen type I alpha 1
COL4A1	collagen type IValpha 1
COL5A1	collagen type V alpha 1
EAE	experimental autoimmune encephalomyelitis
ECM	extracellular matrix
EMT	epithelial to mesenchymal transition
FN	fibronectin

GFAP	glial fibrillary acidic protein
KO	knock-out
MOG	myelin oligodendrocyte glycoprotein
MS	multiple sclerosis
NAGM	normal-appearing gray matter
NAWM	normal-appearing white matter
PVS	perivascular space
RGC-32	response gene to complement 32
ROCK	rho-associated coiled-coil-containing protein kinase
WT	wild-type

References

1. Badea TC, Niculescu FI, Soane L, Shin ML, Rus H. Molecular cloning and characterization of RGC-32, a novel gene induced by complement activation in oligodendrocytes. J Biol Chem. 1998;273:26977–81. [PubMed: 9756947]
2. Badea T, Niculescu F, Soane L, Fosbrink M, Sorana H, Rus V, et al. RGC-32 increases p34CDC2 kinase activity and entry of aortic smooth muscle cells into S-phase. J Biol Chem. 2002;277:502–8. [PubMed: 11687586]
3. Vlaicu SI, Tatomir A, Boodhoo D, Ito T, Fosbrink M, Cudrici C, et al. RGC-32 is expressed in the human atherosclerotic arterial wall: role in C5b-9-induced cell proliferation and migration. Exp Mol Pathol. 2016;101:221–30. [PubMed: 27619159]
4. Fosbrink M, Cudrici C, Tegla CA, Soloviova K, Ito T, Vlaicu S, et al. Response gene to complement 32 is required for C5b-9 induced cell cycle activation in endothelial cells. Exp Mol Pathol. 2009;86: 87–94. [PubMed: 19162005]
5. Rus H, Cudrici C, Niculescu F, Shin ML. Complement activation in autoimmune demyelination: dual role in neuroinflammation and neuroprotection. J Neuroimmunol. 2006;180:9–16. [PubMed: 16905199]
6. Tegla CA, Cudrici CD, Azimzadeh P, Singh AK, Trippe R, 3rd, Khan A, et al. Dual role of response gene to complement-32 in multiple sclerosis. Exp Mol Pathol. 2013;94:17–28. [PubMed: 23000427]
7. Rus V, Nguyen V, Tatomir A, Lees JR, Mekala AP, Boodhoo D, et al. RGC-32 promotes Th17 cell differentiation and enhances experimental autoimmune encephalomyelitis. J Immunol. 2017;198: 3869–77. [PubMed: 28356385]
8. Vlaicu SI, Cudrici C, Ito T, Fosbrink M, Tegla CA, Rus V, et al. Role of response gene to complement 32 in diseases. Arch Immunol Ther Exp. 2008;56:115–22.
9. Huang W-Y, Li Z-G, Rus H, Wang X, Jose PA, Chen S-Y. RGC-32 mediates transforming growth factor-β-induced epithelialmesenchymal transition in human renal proximal tubular cells. J Biol Chem. 2009;284:9426–32. [PubMed: 19158077]
10. Guo X, Jose PA, Chen S-Y. Response gene to complement 32 interacts with Smad3 to promote epithelial–mesenchymal transition of human renal tubular cells. Am J Physiol Cell Physiol. 2011;300: C1415–C21. [PubMed: 21307346]
11. Sofroniew MV. Astrogliosis. Cold Spring Harb Perspect Biol. 2015;7:a020420.
12. Voskuhl RR, Peterson RS, Song B, Ao Y, Morales LB, Tiwari-Woodruff S, et al. Reactive astrocytes form scar-like perivascular barriers to leukocytes during adaptive immune inflammation of the CNS. J Neurosci. 2009;29:11511–22. [PubMed: 19759299]

13. Anderson MA, Ao Y, Sofroniew MV. Heterogeneity of reactive astrocytes. Neurosci Lett. 2014;565:23–9. [PubMed: 24361547]
14. Zamanian JL, Xu L, Foo LC, Nouri N, Zhou L, Giffard RG, et al. Genomic analysis of reactive astrogliosis. J Neurosci. 2012;32: 6391–410. [PubMed: 22553043]
15. Cudrici C, Ito T, Zafranskaia E, Weerth S, Rus V, Chen H, et al. Complement C5 regulates the expression of insulin-like growth factor binding proteins in chronic experimental allergic encephalomyelitis. J Neuroimmunol. 2008;203:94–103. [PubMed: 18692252]
16. Tegla CA, Azimzadeh P, Andrian-Albescu M, Martin A, Cudrici CD, Trippe R, 3rd, et al. SIRT1 is decreased during relapses in patients with multiple sclerosis. Exp Mol Pathol. 2014;96:139–48. [PubMed: 24397908]
17. Hoffman WH, Cudrici CD, Zafranskaia E, Rus H. Complement activation in diabetic ketoacidosis brains. Exp Mol Pathol. 2006;80:283–8. [PubMed: 16494864]
18. Rus HG, Kim LM, Niculescu FI, Shin ML. Induction of C3 expression in astrocytes is regulated by cytokines and Newcastle disease virus. J Immunol. 1992;148:928–33. [PubMed: 1530957]
19. Tegla CA, Cudrici CD, Nguyen V, Danoff J, Kruszewski AM, Boodhoo D, et al. RGC-32 is a novel regulator of the T-lymphocyte cell cycle. Exp Mol Pathol. 2015;98:328–37. [PubMed: 25770350]
20. Rus HG, Niculescu F, Shin ML. Sublytic complement attack induces cell cycle in oligodendrocytes. J Immunol. 1996;156:4892–900. [PubMed: 8648139]
21. Mohan H, Krumbholz M, Sharma R, Eisele S, Junker A, Sixt M, et al. Extracellular matrix in multiple sclerosis lesions: fibrillar collagens, biglycan and decorin are upregulated and associated with infiltrating immune cells. Brain Pathol. 2010;20:966–75. [PubMed: 20456365]
22. Moreels M, Vandenabeele F, Dumont D, Robben J, Lambrichts I. Alpha-smooth muscle actin (alpha-SMA) and nestin expression in reactive astrocytes in multiple sclerosis lesions: potential regulatory role of transforming growth factor-beta 1 (TGF-beta1). Neuropathol Appl Neurobiol. 2008;34:532–46. [PubMed: 18005096]
23. Derynck R, Zhang YE. Smad-dependent and Smad-independent pathways in TGF-beta family signalling. Nature. 2003;425:577–84. [PubMed: 14534577]
24. Jinnin M, Ihn H, Tamaki K. Characterization of SIS3, a novel specific inhibitor of Smad3, and its effect on transforming growth factor-beta1-induced extracellular matrix expression. Mol Pharmacol. 2006;69:597–607. [PubMed: 16288083]
25. Chen S, Crawford M, Day RM, Briones VR, Leader JE, Jose PA, et al. RhoA modulates Smad signaling during transforming growth factor-beta-induced smooth muscle differentiation. J Biol Chem. 2006;281:1765–70. [PubMed: 16317010]
26. Kuivaniemi H, Tromp G, Prockop DJ. Mutations in fibrillar collagens (types I, II, III, and XI), fibril-associated collagen (type IX), and network-forming collagen (type X) cause a spectrum of diseases of bone, cartilage, and blood vessels. Hum Mutat. 1997;9: 300–15. [PubMed: 9101290]
27. Marjamaa J, Tulamo R, Abo-Ramadan U, Hakovirta H, Frosen J, Rahkonen O, et al. Mice with a deletion in the first intron of the Col1a1 gene develop dissection and rupture of aorta in the absence of aneurysms: high-resolution magnetic resonance imaging, at 4.7 T, of the aorta and cerebral arteries. Magn Reson Med. 2006;55: 592–7. [PubMed: 16453315]
28. van Horssen J, Dijkstra CD, de Vries HE. The extracellular matrix in multiple sclerosis pathology. J Neurochem. 2007;103:1293–301. [PubMed: 17854386]
29. Hara M, Kobayakawa K, Ohkawa Y, Kumamaru H, Yokota K, Saito T, et al. Interaction of reactive astrocytes with type I collagen induces astrocytic scar formation through the integrin–N-cadherin pathway after spinal cord injury. Nat Med. 2017;23:818–28. [PubMed: 28628111]
30. Liesi P, Kauppila T. Induction of type IV collagen and other basement-membrane-associated proteins after spinal cord injury of the adult rat may participate in formation of the glial scar. Exp Neurol. 2002;173:31–45. [PubMed: 11771937]
31. Zhu D, Tapadia MD, Palispis W, Luu M, Wang W, Gupta R. Attenuation of robust glial scar formation facilitates functional recovery in animal models of chronic nerve compression injury. J Bone Joint Surg Am. 2017;99:e132. [PubMed: 29257018]
32. Xia M, Zhu Y. Fibronectin enhances spinal cord astrocyte proliferation by elevating P2Y1 receptor expression. J Neurosci Res. 2014;92:1078–90. [PubMed: 24687862]

33. van Horssen J, Vos CM, Admiraal L, van Haastert ES, Montagne L, van der Valk P, et al. Matrix metalloproteinase-19 is highly expressed in active multiple sclerosis lesions. Neuropathol Appl Neurobiol. 2006;32:585–93. [PubMed: 17083473]

34. Massagué J, Wotton D. Transcriptional control by the TGF-β/Smad signaling system. EMBO J. 2000;19:1745–54. [PubMed: 10775259]

35. Zhao P, Gao D, Wang Q, Song B, Shao Q, Sun J, et al. Response gene to complement 32 (RGC-32) expression on M2-polarized and tumor-associated macrophages is M-CSF-dependent and enhanced by tumor-derived IL-4. Cell Mol Immunol. 2015;12:692–9. [PubMed: 25418473]

36. Cregg JM, DePaul MA, Filous AR, Lang BT, Tran A, Silver J. Functional regeneration beyond the glial scar. Exp Neurol. 2014;253:197–207. [PubMed: 24424280]

37. Harlow DE, Macklin WB. Inhibitors of myelination: ECM changes, CSPGs and PTPs. Exp Neurol. 2014;251:39–46. [PubMed: 24200549]

38. Kawano H, Kimura-Kuroda J, Komuta Y, Yoshioka N, Li HP, Kawamura K, et al. Role of the lesion scar in the response to damage and repair of the central nervous system. Cell Tissue Res. 2012;349:169–80. [PubMed: 22362507]

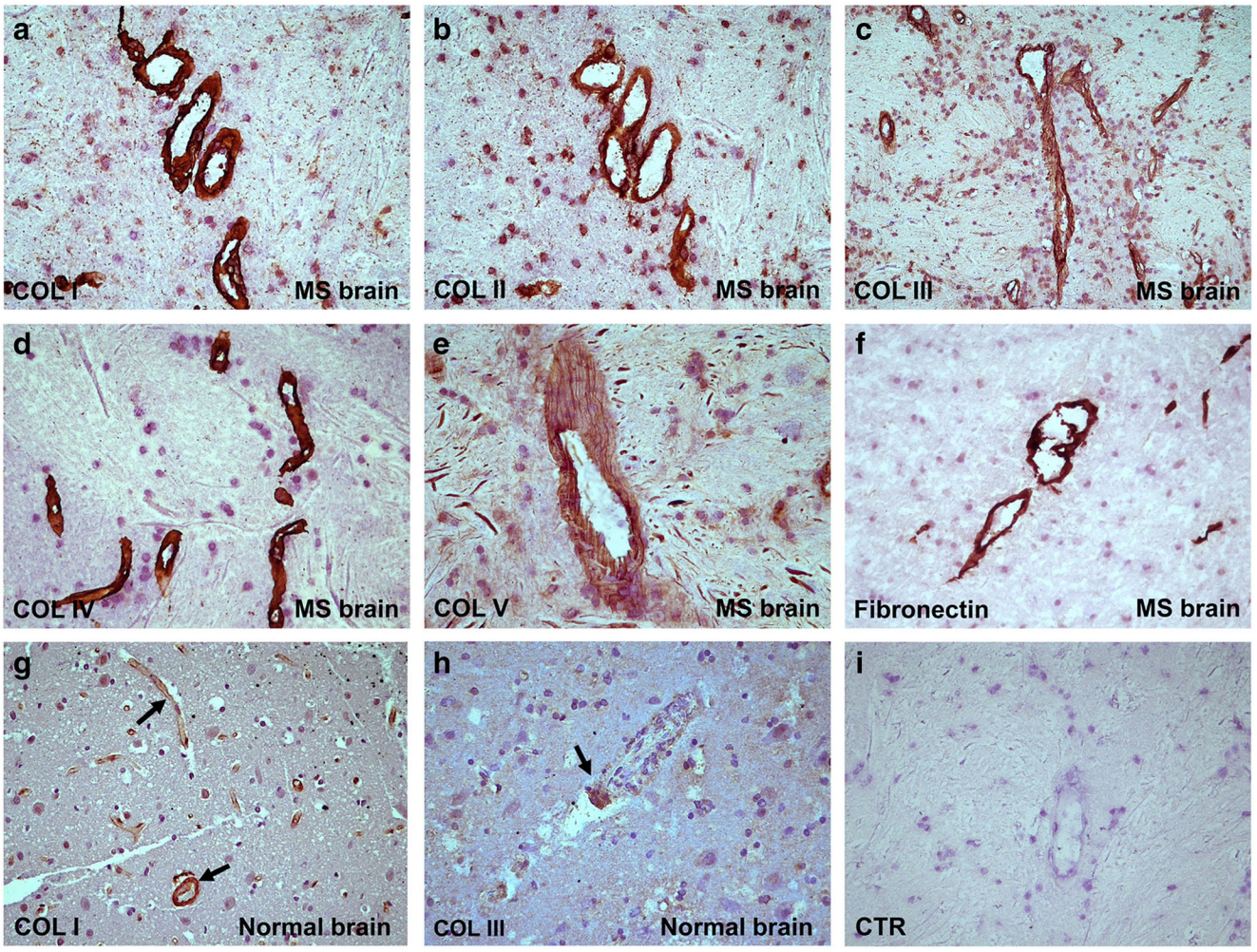

Fig. 1.

Localization of ECM components in MS plaque. Collagen I (**a**), collagen II (**b**), collagen III (**c**), collagen IV (**d**), collagen V (**e**), and fibronectin (**f**) were localized by immunostaining in MS plaques, around the blood vessels and in the parenchyma. Collagens I, III, IV, and V form a meshwork in the perivascular space in MS plaques. In active lesions, collagen V is found around blood vessels and in the perivascular space as well as in parenchymal areas outside the PVS (**e**). In the normal brain, collagen I (**g**) and collagen III (**h**) were detected at significantly lower levels than in MS plaques. Control for the immunoperoxidase reaction was negative (**i**). Nova RED was used as a substrate for immunostaining and hematoxylin for counter staining. Original magnifications: (**a**)–(**d**) and (**f**)–(**i**): × 200, (**e**): × 400

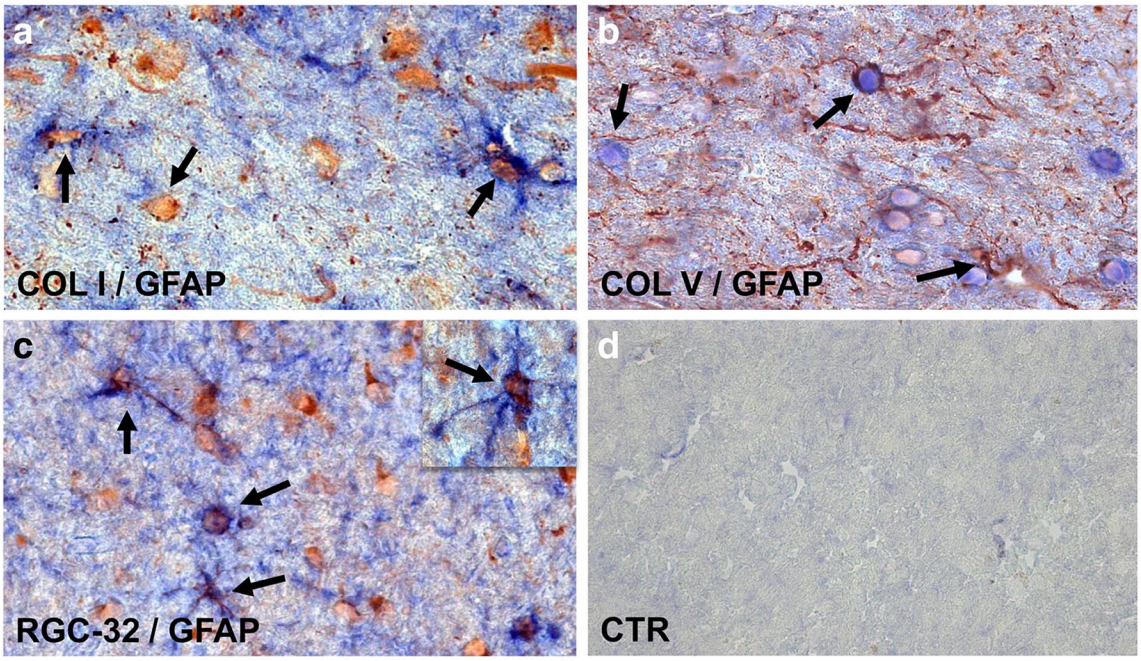

Fig. 2.

Co-localization of collagens I and V and RGC-32 with GFAP. Collagens I (**a**), V (**b**), and RGC-32 (**c**) were found to be co-localized with $GFAP^+$ astrocytes in parenchymal areas (arrows) of MS plaques. Control for the immunoperoxidase reaction was negative (**d**). Collagen I (red) and GFAP (blue) in (**a**); collagen V (blue) and GFAP (red) in (**b**); RGC-32 (red) and GFAP (blue) in (**c**). Original magnification: (**a**)–(**c**): × 400, (**d**): × 200

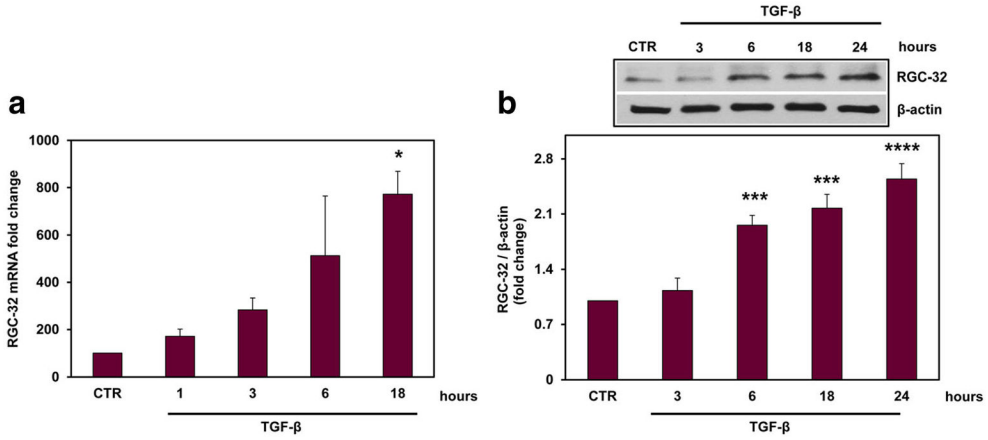

Fig. 3.

TGF-β induces the expression of RGC-32 in astrocytes. Rat astrocytes were cultured and stimulated with TGF-β (10 ng/ml) for the indicated periods of time. RGC-32 mRNA expression was quantified by real-time PCR (**a**) and was normalized to that of 18S RNA. The results are presented as fold increase over unstimulated (CTR), which was considered to be 100%. RGC-32 protein expression was quantified by Western blotting and normalized to β-actin (**b**), and the results are presented as fold increase over unstimulated (CTR). A representative blot is shown. Both RGC-32 mRNA and protein were induced by TGF-β. Results are expressed as mean ± SEM ($n = 3$). *$p < 0.05$; ***$p < 0.001$; ****$p < 0.0001$

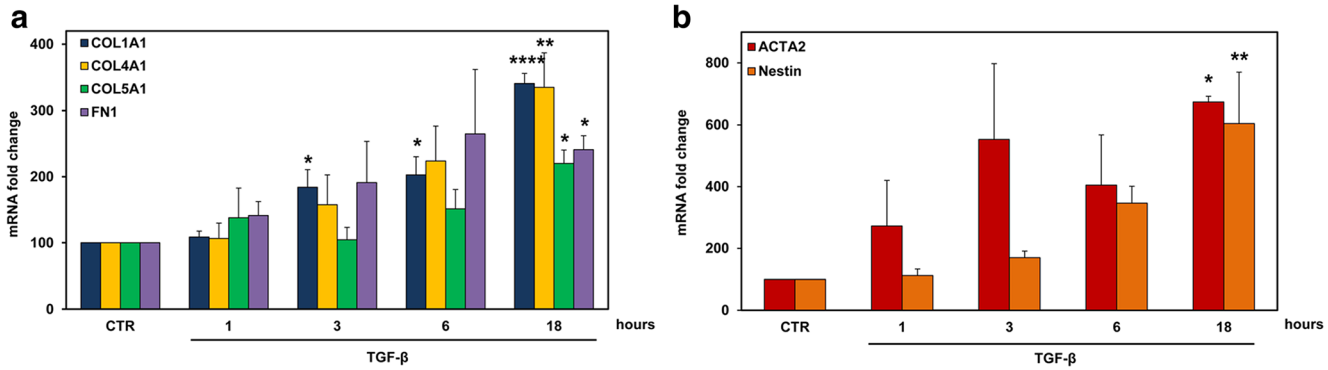

Fig. 4.

TGF-β induces the expression of COL1A1, COL4A1, COL5A1, FN1, ACTA2, and nestin mRNAs in astrocytes. Rat astrocytes were exposed to TGF-β (10 ng/ml) for the indicated periods of time. Expression of COL1A1, COL4A1, COL5A1, FN1 (**a**), ACTA2, and nestin (**b**) was determined by real-time PCR and normalized to that of 18S RNA. The results are presented as fold increase over unstimulated (CTR), which was considered to be 100. Results are expressed as mean ± SEM ($n = 3$). *$p < 0.05$; **$p < 0.01$; ****$p < 0.0001$

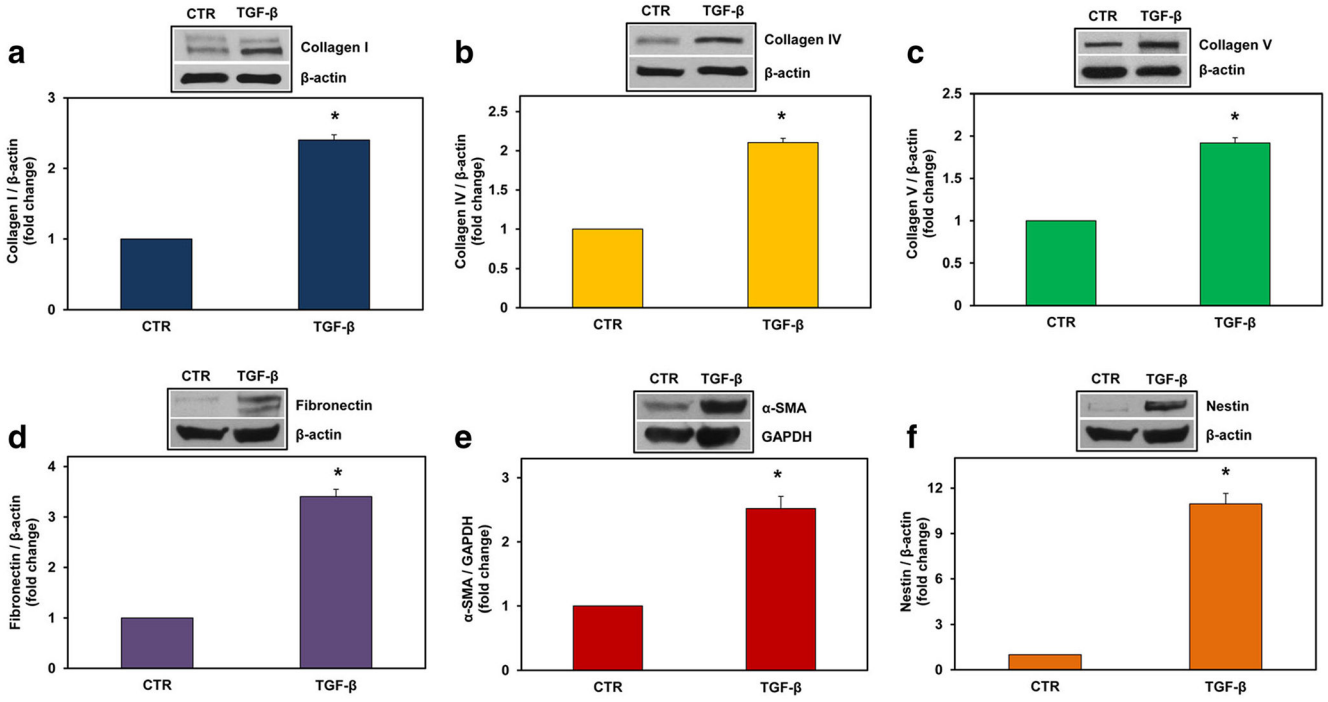

Fig. 5.

TGF-β induces the expression of collagen type I, IV, V, fibronectin, α-SMA, and nestin proteins in astrocytes. Rat astrocytes were exposed to TGF-β (10 ng/ml) for 24 h. Expression of collagen I (**a**), collagen IV (**b**), collagen V (**c**), fibronectin (**d**), α-SMA (**e**), and nestin (**f**) was detected by Western blotting and was normalized to β-actin, except in (**e**), where it was normalized to GAPDH. The results are presented as fold increase over unstimulated (CTR), which was considered to be 1. Results are expressed as mean ± SEM ($n = 3$). A representative blot for each component is shown. *$p < 0.05$

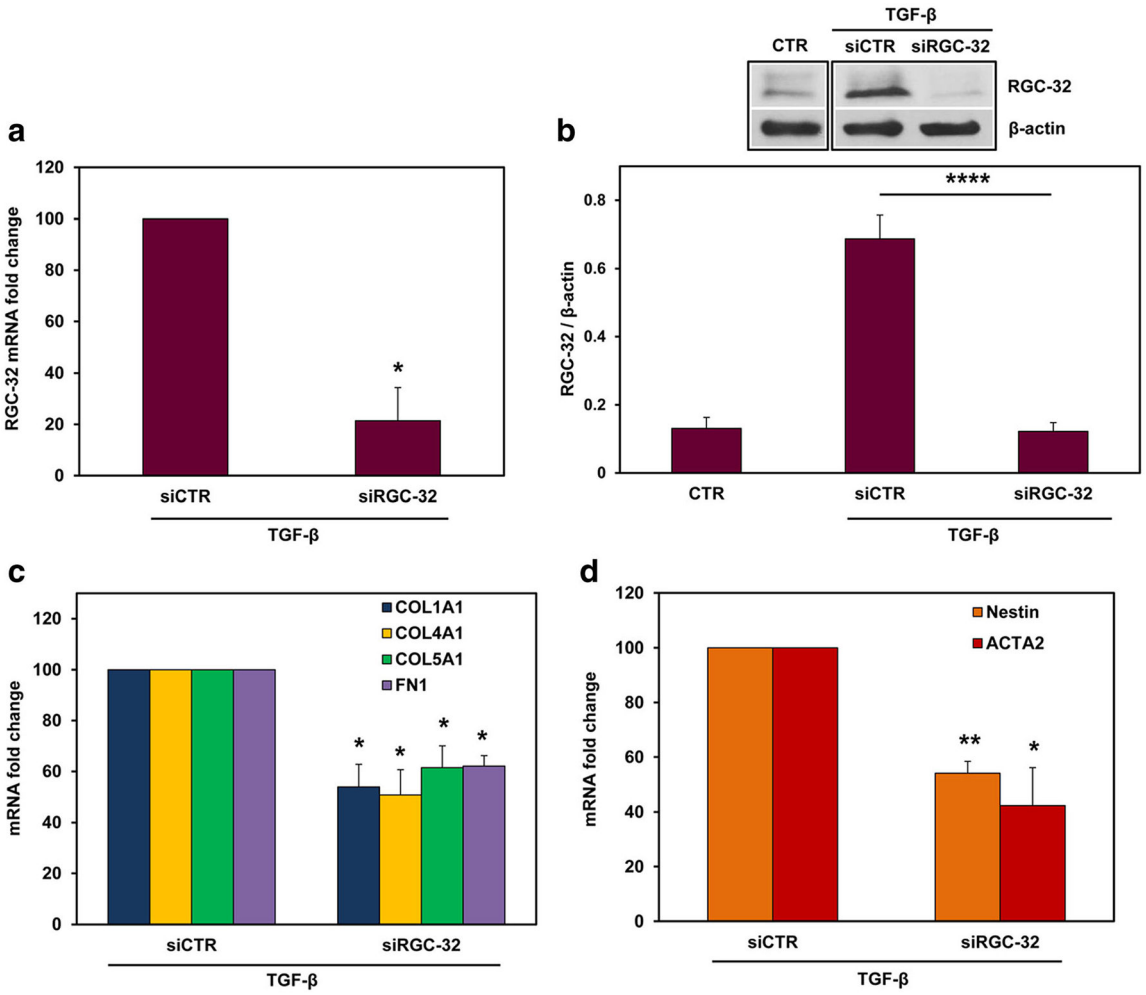

Fig. 6.

Effect of RGC-32 silencing on COL1A1, COL4A1, COL5A1, FN1, ACTA2, and nestin mRNAs in astrocytes. Cultured rat astrocytes were transfected with siRGC-32 or siCTR using Lipofectamine 3000 and then stimulated with TGF-β (10 ng/ml) for 18 h. RGC-32 silencing significantly reduced both RGC-32 mRNA (**a**) and protein expression (**b**) after TGF-β treatment, as compared to siCTR expression. RGC-32 silencing significantly reduced the TGF-β-induced mRNA expression of COL1A1, COL4A1, COL5A1, FN1 (**c**), ACTA2, and nestin (**d**) when compared with that of siCTR. mRNA expression was normalized to 18S RNA, and the results are shown as fold change over siCTR, which was considered to be 100% (**a, c, d**). The protein expression in (**b**) is shown as ratio to β-actin. Results are expressed as mean ± SEM ($n = 3$). *$p < 0.05$; **$p < 0.01$; ****$p < 0.0001$

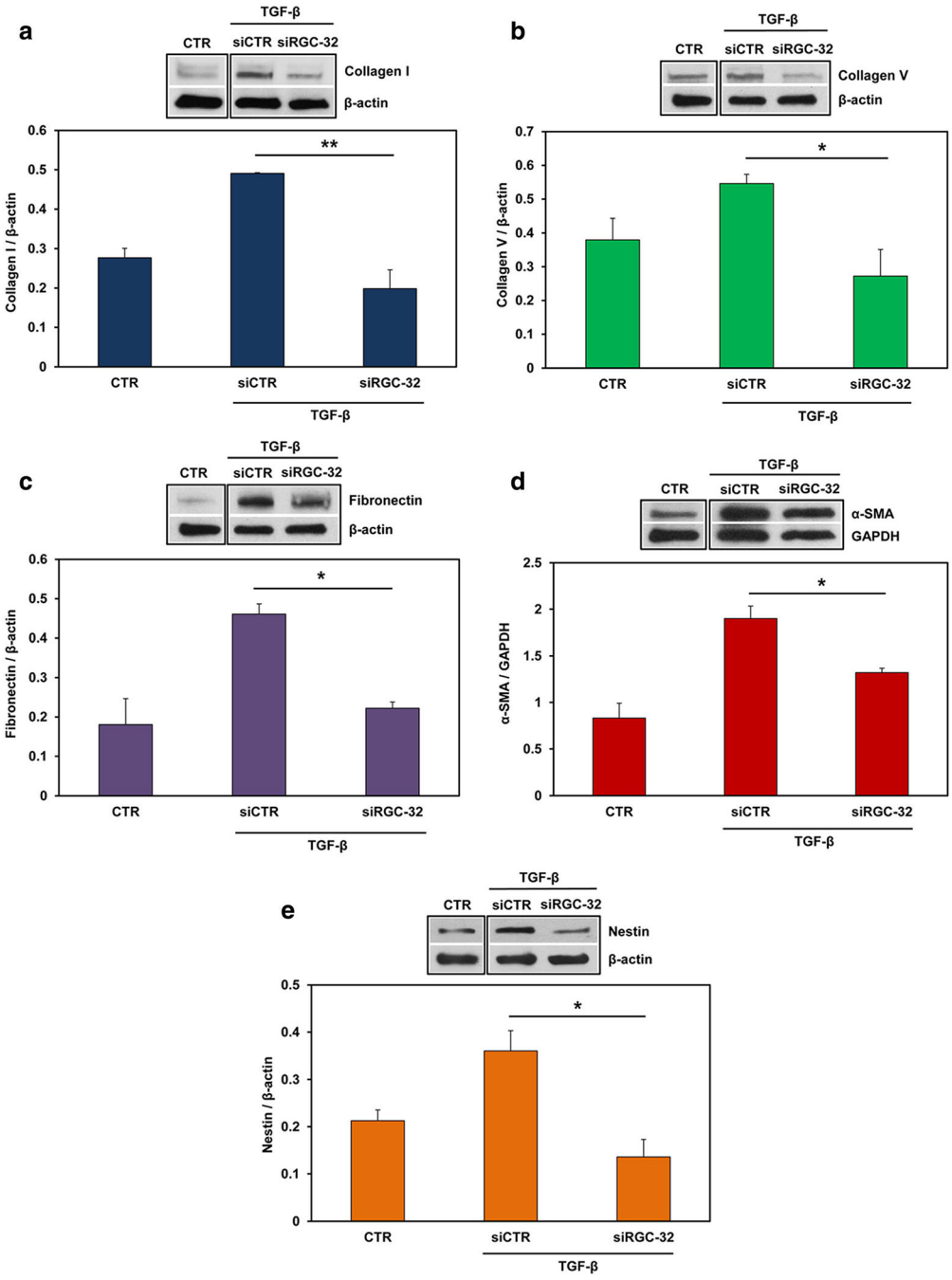

Fig. 7.

Effect of RGC-32 silencing on ECM proteins, α-SMA, and nestin in astrocytes. Cultured rat astrocytes were transfected with siRGC-32 or siCTR using Lipofectamine 3000, then stimulated with TGF-β (10 ng/ml) for 24 h. RGC-32 silencing significantly reduced the protein expression of collagen I (a), collagen V (**b**), fibronectin (**c**), α-SMA (**d**), and nestin (**e**) when compared with that of siCTR. The protein expression was normalized to β-actin, except in (**d**), where it was normalized to GAPDH. A representative blot for each component is shown. Results are expressed as mean ± SEM ($n = 3$). *$p < 0.05$; **$p < 0.01$

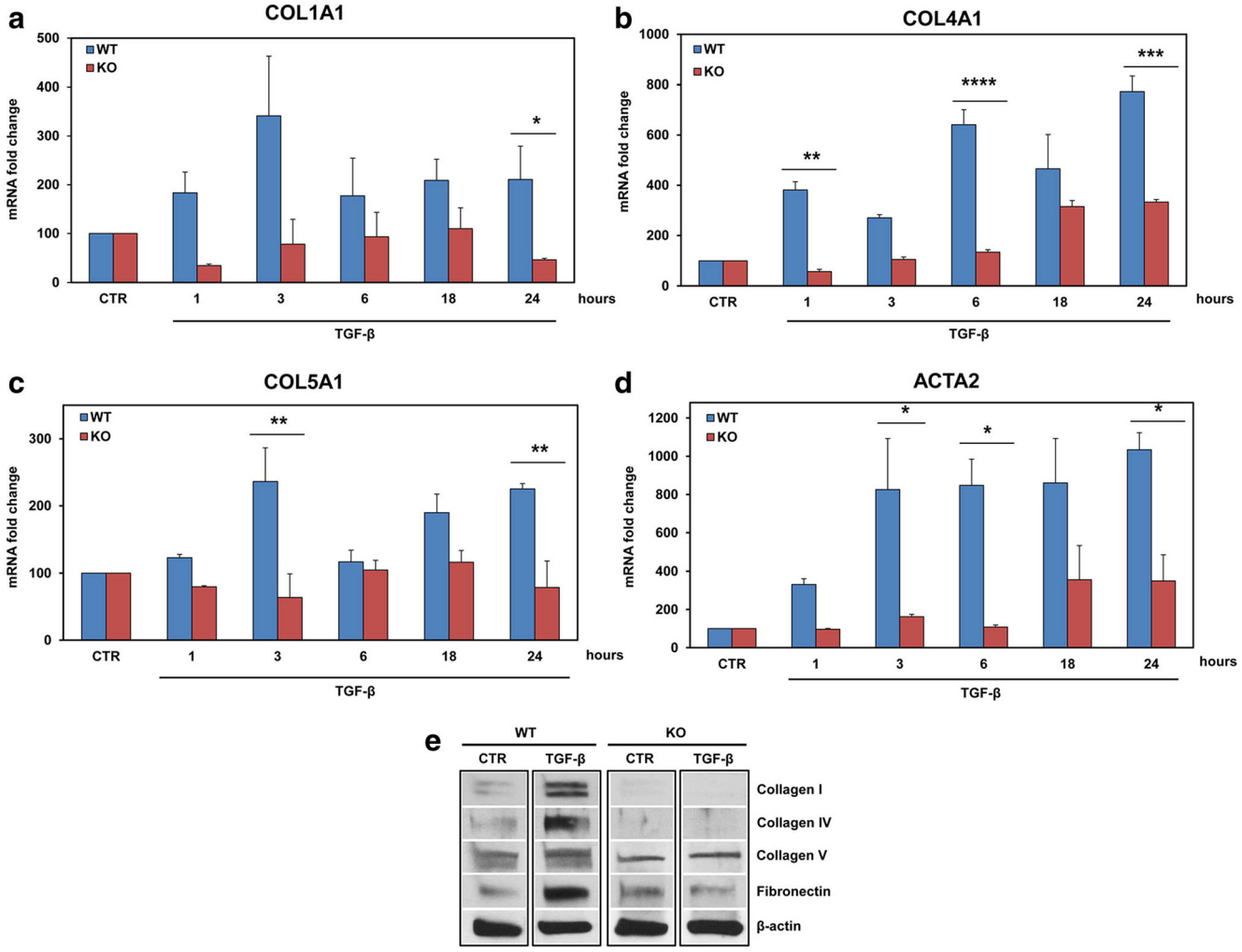

Fig. 8.

Effect of TGF-β on ECM components and α-SMA expression in RGC-32$^{-/-}$ astrocytes. Primary astrocytes cultures from WT and RGC-32$^{-/-}$ neonatal mice were stimulated with TGF-β (10 ng/ml) for the indicated periods of time, and the total mRNA was purified and analyzed for the expression of COL1A1 (**a**), COL4A1 (**b**), COL5A1 (**c**), and ACTA2 (**d**). The TGF-β-induced expression of these transcripts was significantly reduced in RGC-32$^{-/-}$ mice when compared to the WT mice. After 24 h of TGF-β stimulation (10 ng/ml), total proteins were purified and the expression of collagen I, collagen IV, collagen V, and fibronectin was analyzed by Western blotting. A representative blot for each component is shown (**e**). mRNA expression was normalized to that of 18S RNA, and the results are shown as fold change over unstimulated (CTR), which was considered to be 100. Data are expressed as mean ± SEM ($n = 3$). *$p < 0.05$; **$p < 0.01$; ***$p < 0.001$; ****$p < 0.0001$

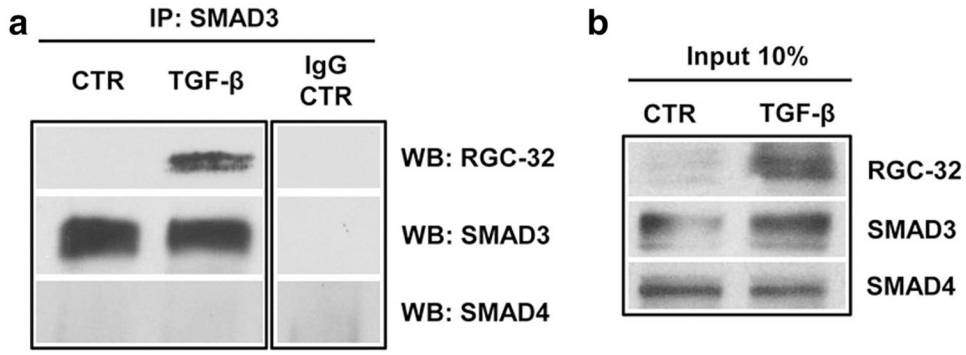

Fig. 9.

RGC-32 physically interacts with Smad3 in astrocytes. Primary rat astrocytes were treated with vehicle (CTR) or TGF-β (10 ng/ml) for 24 h, and co-immunoprecipitation was performed. Control IgG and anti-Smad3 antibodies were used for immunoprecipitation (IP); anti-RGC-32, -SMAD3 and -SMAD4 antibodies were used for Western blotting (WB). Only Smad3 physically interacted with RGC-32 in astrocytes, and only after stimulation with TGF-β (**a**). Input is shown in (**b**)

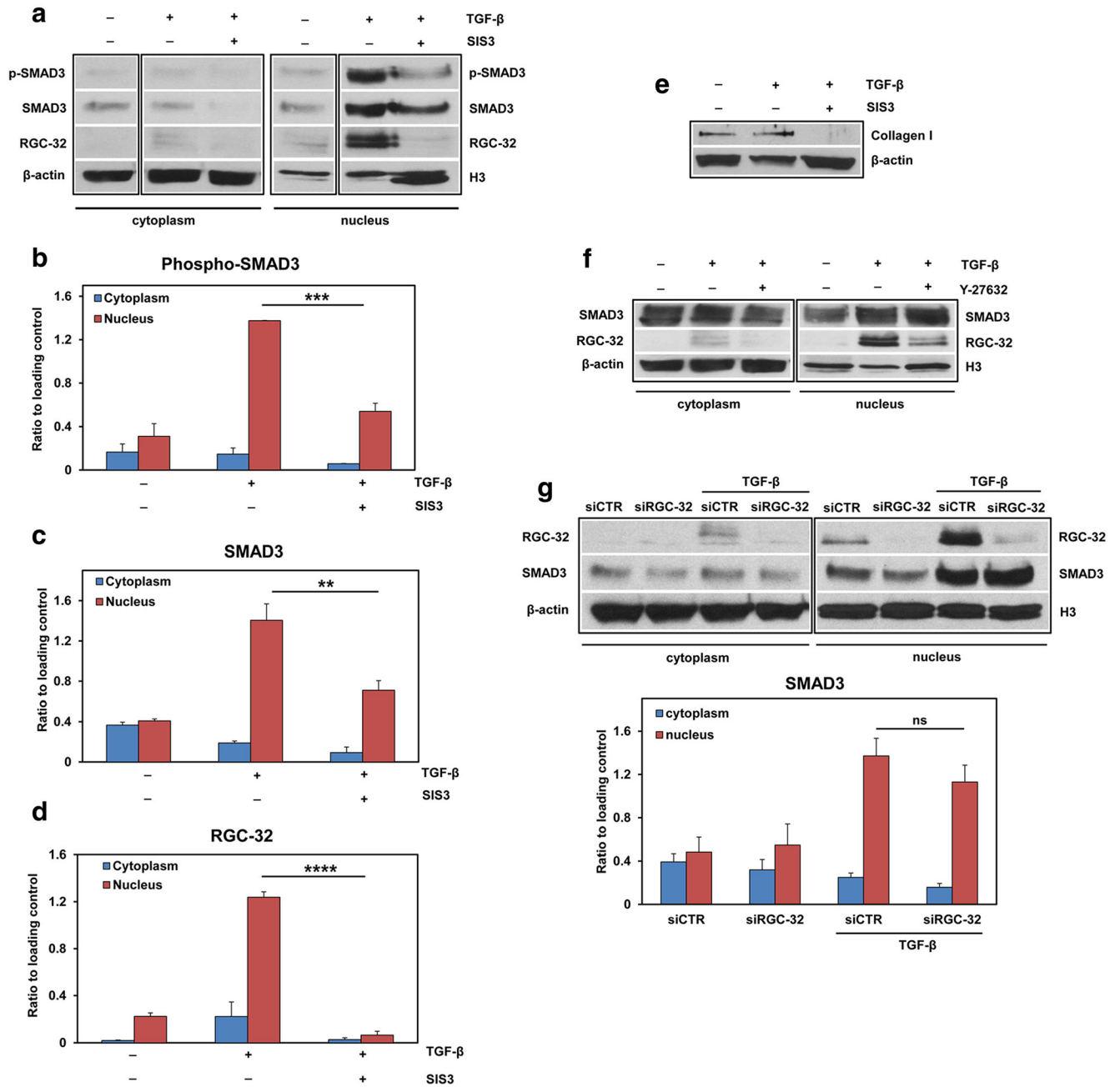

Fig. 10.

RGC-32 nuclear translocation depends on Smad3 phosphorylation and ROCK activation. Primary rat astrocytes were pre-treated with SIS3 (10 μM), which suppresses Smad3 phosphorylation without affecting the MAPK/p38, ERK, or PI3-kinase signaling pathways, and with Y-27362 (10 μM), an inhibitor of the Rho-associated, coiled-coil-containing protein kinase (ROCK). The cells were then stimulated with TGF-β (10 ng/ml) for 4 h. Cell lysates were separated into cytoplasmic and nuclear fractions and then processed by Western blotting. TGF-β treatment resulted in nuclear translocation of phosphorylated Smad3, total Smad3 and RGC-32 (**a–d**). RGC-32 nuclear translocation was significantly reduced after

treatment with SIS3 (**a, d**). A representative blot for each component is shown in (**a**). SIS3 also significantly reduced TGF-β-induced collagen I expression (**e**). Y-27362 treatment also reduced RGC-32 nuclear translocation, whereas Smad3 remained unaffected after the same treatment (**f**). A representative blot for each component is shown in (**f**). On the other hand, siRNA-mediated RGC-32 knock-down did not affect the nuclear translocation of Smad3 (**g**). The results are expressed as ratios to β-actin for the cytoplasmic fraction and to histone H3 for the nuclear fraction. Data in (**b**), (**c**), (**d**), and (**g**) are shown as mean ± SEM ($n = 3$). **$p < 0.01$; ***$p < 0.001$; ****$p < 0.0001$; ns = not statistically significant

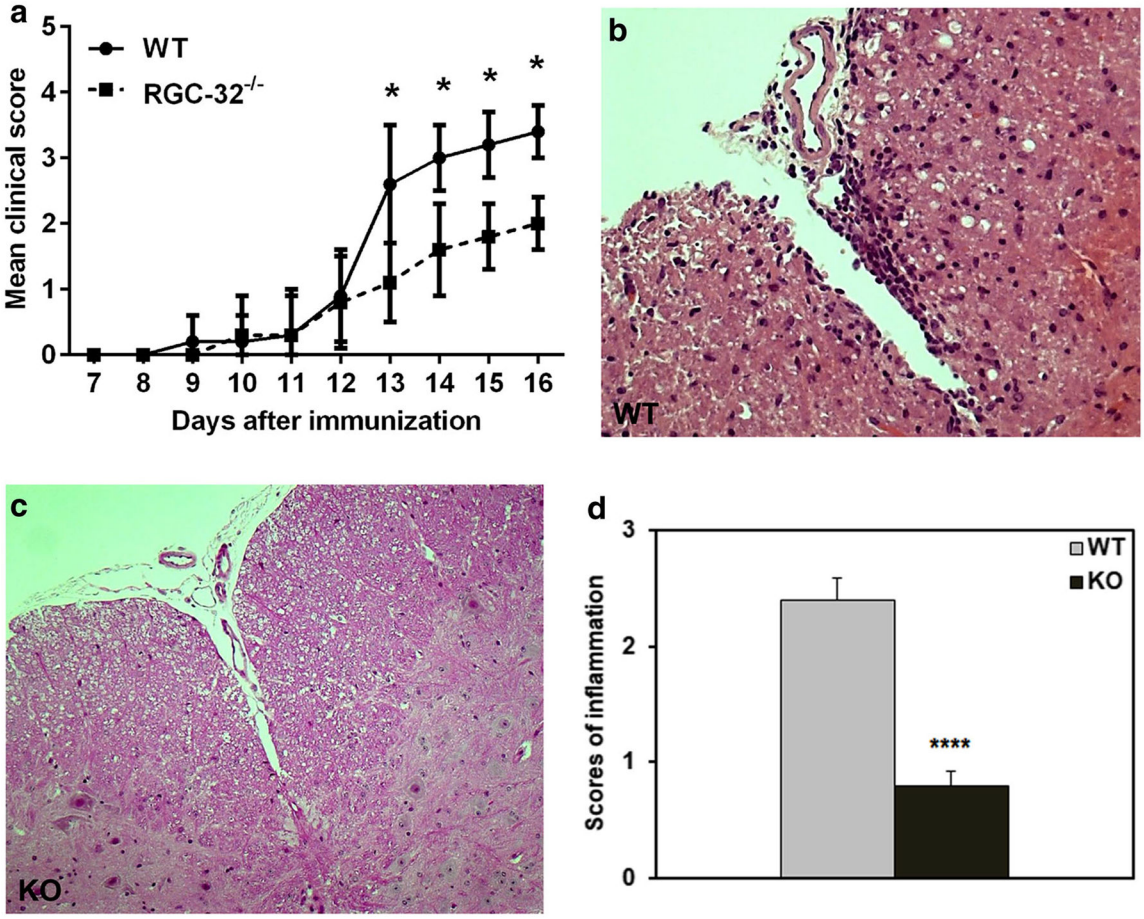

Fig. 11.

RGC-32 deficiency attenuates the clinical course of EAE and CNS infiltration. WT and RGC-32$^{-/-}$ mice were immunized with $MOG_{35–55}$ and then scored for EAE. Means ± SEM of clinical EAE scores representative of three independent experiments (5 mice for each group/experiment) are shown in (**a**). Cervical spinal cords were harvested at the peak of disease from WT (**b**) and KO (**c**) mice and stained with hematoxylin and eosin. KO mice showed fewer inflammatory infiltrates than did WT mice. Original magnification: × 200. **d** The score for inflammation in RGC-32$^{-/-}$ was decreased to 0.8 ± 0.1 when compared with WT mice (2.4 ± 0.18) (****$p < 0.0001$)

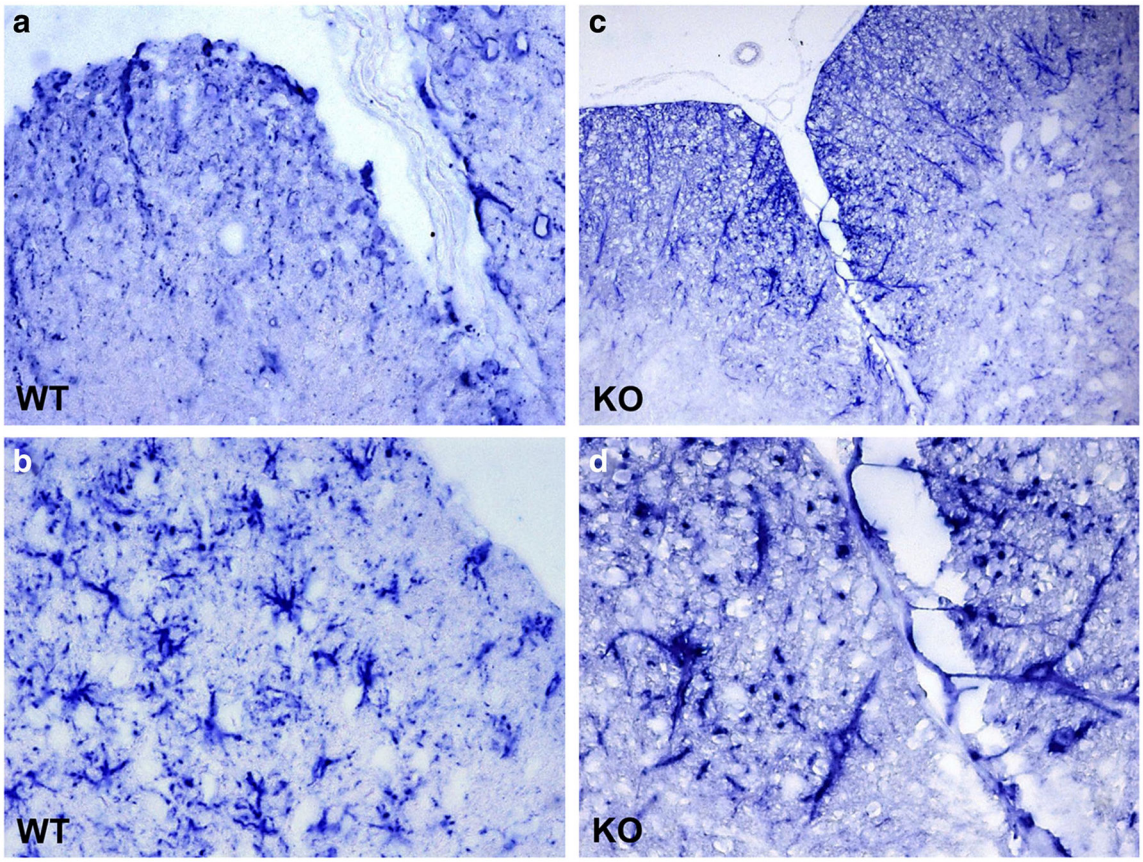

Fig. 12.

Lack of RGC-32 affects astrocyte morphology in EAE. Cervical spinal cords were harvested at the peak of disease from WT (**a, b**) and KO (**c, d**) mice and stained with anti-GFAP antibody. The color reaction was developed using an alkaline phosphatase substrate kit. In the presence of RGC-32, astrocytes adopted a reactive phenotype with body hypertrophy, but the lack of RGC-32 resulted in elongated astrocyte morphology. Original magnification: (**a**) and (**c**): × 200, (**b**) and (**d**): × 400

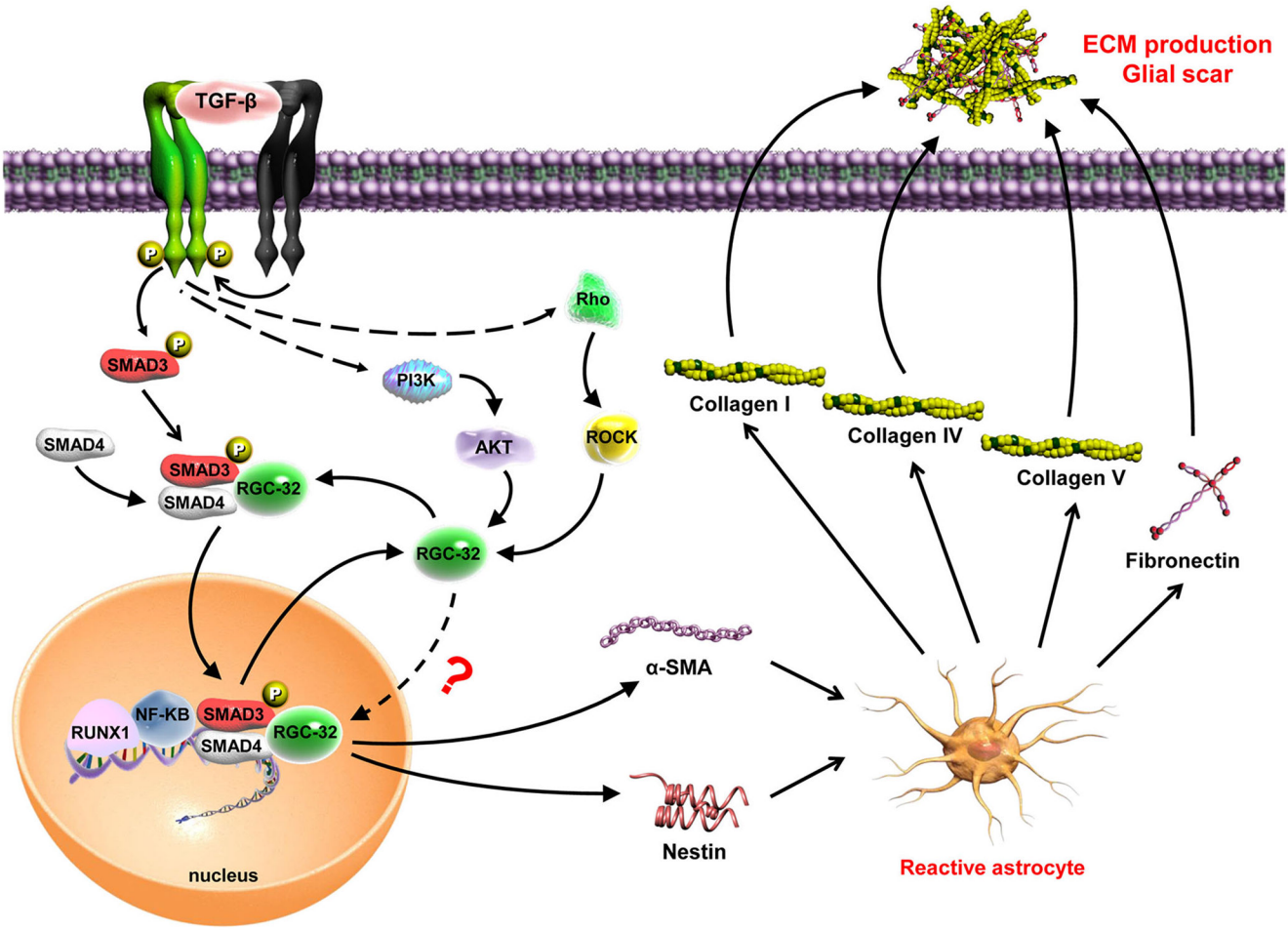

Fig. 13.

Schematic representation of the role of RGC-32 in TGF-β induced extracellular matrix production by astrocytes. Our data show that after TGF-β stimulation RGC-32 expression is increased. RGC-32 physically interacts with Smad3 and is transferred to the nucleus, a process which requires Smad3 phosphorylation. Rho-associated, coiled-coil-containing protein kinase (ROCK) seems also to play an important in RGC-32 nuclear translocation. Our previous results show that RGC-32 transcription in astrocytes is regulated by RUNX1 and NF-κB transcription factors which may be recruited at RGC-32 promoter by Smad3 complexes. Once its expression induced, RGC-32 mediates the production of reactive astrocyte markers nestin and α-SMA, as well as the extracellular matrix components collagen I, collagen IV, collagen V, and fibronectin. These data suggest that RGC-32 plays an important role in TGF-β-induced gliosis

Table 1

Localization of collagen and fibronectin in multiple sclerosis and control brains

Case number (age, sex)	Lesion (number)	Lesion type	Collagen 1		Collagen 2		Collagen 3		Collagen 4		Collagen 5		Fibronectin	
			PA	V/PV	PA	V/PV	PA	V/PV	PA	V/PV	PA	V/PV	PA	V/PV
1 (53, F)	Occipital (3)	Plaque	++	++	++	++	+	+++	++	+++	++	+/++	++	++
		NAWM	++	++	++	+++	+/++	++/+++	−	++	++/+++	++	++	++
		NAGM	+++	++	+	+/++	+/++	++	−	+++	++	++	+++	++
	Parietal (1)	Plaque	+++	+++	+++	++	+++	+	+++	+++	++	++	+++	+++
2 (68, M)	Parietal (2)	Plaque	+++	+++	+	+	ND	ND	+++	+++	+++	+++	+++	+++
		NAWM	++	+++	+++	+++	++	+++	+++	+++	+++	+++	++	+++
3 (62, M)	Parietal (3)	Plaque	+++	+++	++	++	+	++	++	+++	++	++	+	++
		NAWM	+	+++	ND	ND	++	+++	+	++	+	++	ND	ND
		NAGM	ND	ND	ND	ND	+++	+++	ND	ND	ND	ND	ND	ND
4 (38, F)	Frontal (2)	Plaque	+/++	++	++/+++	+++	+	++	++	+++	+	++	+	++
		NAGM	ND	ND	ND	ND	+++	+	ND	ND	−	+	ND	ND
5 (47, F)	Parietal (2)	Plaque	+++	++	+	++	+	++	+	++/+++	+/++	++	++	++
		NAGM	ND	ND	ND	ND	+/++	+/++	ND	ND	+	+	ND	ND
	Frontal (3)	Plaque	++	+++	+	+++	+/++	+++	+++	+++	++	++	+	++
		NAWM	+	+	+/++	++	++	++/+++	−	+++	++	+/++	+	++
		NAGM	+ /−	++	ND	ND	++	+++	+	+++	+++	++	ND	ND
6 (50, M)	Temporal (2)	Plaque	+	++	+	++	+	++	+	++	+	+/++	+++	++
		NAGM	+++	+	ND	ND	−	++	−	+	+	+	+++	+
7 (51, F)	Frontal (1)	Plaque	+/++	+++	++	+++	++	+++	+++	+++	+++	+++	++	+
8–13	Normal (8)	Control WM	−	+	−	+	−	+	−	+	−	+	ND	ND

F female, *M* male, *NAWM* normal-appearing white matter, *NAGM* normal-appearing gray matter, *ND* non-determined, − negative, + slightly positive, ++ positive, +++ highly positive, *PA* parenchymal, *V/PV* vascular/perivascular